

***Final Draft***  
**of the original manuscript:**

Li, Y.; Pyczak, F.; Paul, J.; Oehring, M.; Lorenz, U.; Yao, Z.; Ning, Y.:  
**Rafting of Gamma' precipitates in a Co-9Al-9W superalloy during  
compressive creep**

In: Materials Science and Engineering A 719 (2018) 43 - 48

First published online by Elsevier: February 8, 2018

DOI: 10.1016/j.msea.2018.02.017

<https://dx.doi.org/10.1016/j.msea.2018.02.017>

# Rafting of $\gamma'$ precipitates in a Co-9Al-9W superalloy during compressive creep

Yuzhi Li<sup>a\*</sup>, Florian Pyczak<sup>b</sup>, Jonathan Paul<sup>b</sup>, Michael Oehring<sup>b</sup>, Uwe Lorenz<sup>b</sup>, Zekun Yao<sup>a</sup>, Yongquan Ning<sup>a</sup>

- a. School of Materials Science and Engineering, Northwestern Polytechnical University, 710072 Xi'an, China
- b. Institute of Materials Research, Helmholtz-Zentrum Geesthacht, 21502 Geesthacht, Germany

\*Corresponding author:

Yuzhi Li: [liyuzhiyaya@hotmail.com](mailto:liyuzhiyaya@hotmail.com)

Tel: +86 15929303068; Fax: +86 29 88492642

## Abstract

The rafting of  $\gamma'$  precipitates was investigated in a single crystal of Co-9Al-9W(at%) superalloy after compression creep tests at 850 °C. Scanning electron micrographs show that the  $\gamma'$  precipitates raft perpendicular to the compressive stress axis, due to their positive lattice parameter misfit. The rafting of  $\gamma'$  precipitates occurred after the minimum strain rate was reached. The dislocation structure and stacking faults were investigated by transmission electron microscopy. Dislocations preferentially moved in the horizontal  $\gamma$  matrix channels where they can relieve the coherency stress at horizontal  $\gamma/\gamma'$  interfaces. After extended periods of creep, rafting of the  $\gamma'$  precipitates perpendicular to the external compressive stress axis occurred. The merging of  $\gamma'$  precipitates during rafting initiated at the precipitates corners, leaving pockets of matrix phase in the vertical  $\gamma$  channels between adjacent  $\gamma'$  precipitates. The necessary diffusion of alloying elements during the rafting process between the two orientations of matrix channels should be decelerated as diffusion is slower in the ordered  $L1_2$   $\gamma'$  phase than in the disordered  $\gamma$  phase.

**Keywords:** rafting, coherency stresses, dislocations, stacking faults, diffusion

## 1. Introduction

The novel cobalt-base superalloys with a  $\gamma/\gamma'$  two-phase microstructure recently obtained lots of attention due to their improved hot-corrosion resistance, oxidation resistance and high temperature strength when compared to conventional cobalt-base superalloys<sup>[1-3]</sup>. The Co- $\gamma$  solid solution matrix with an fcc structure and the  $\text{Co}_3(\text{Al,W})-\gamma'$  precipitates with a  $L1_2$  crystal structure possess similar lattice parameters, which promotes coherent interfaces between the matrix and precipitates<sup>[4-6]</sup>. The cubic  $\gamma'$  precipitates are aligned regularly along  $\langle 001 \rangle$  orientations, which is similar to the microstructure and precipitate

morphology of nickel-base superalloys<sup>[7-9]</sup>. However, the Co-Al-W alloys promise a higher service temperature and improved strength at elevated temperatures due to the higher melting point of cobalt. Moreover, these novel cobalt-based superalloys exhibit better single-crystal solidification characteristics compared to nickel-base alloys<sup>[10-13]</sup>.

Creep strength is one of the most important properties for superalloys due to their elevated service temperature loading. The creep deformation in Co-Al-W ternary alloys is associated with the movement of  $a/2\langle 101 \rangle$  type dislocations in the  $\gamma$  matrix in combination with  $a/3\langle 112 \rangle$  superpartials shearing the  $\gamma'$  precipitates and generating stacking faults inside them<sup>[14-16]</sup>. The most significant characteristic during the creep of  $L1_2$  hardened superalloys is that the  $\gamma'$  precipitates can directionally coarsen, forming rafts from the initially cubic  $\gamma'$  particles. It was reported that the applied stress, lattice misfit, and elastic modulus mismatch provide the driving force for this morphology evolution<sup>[17-19]</sup>.

Numerous studies exist concerning the microstructural evolution of single crystal nickel-base superalloys with negative lattice misfits during creep. In such cases, the initially cubic  $\gamma'$  precipitates raft into precipitates that are elongated perpendicular to the tensile stress axis or parallel to the compressive stress axis<sup>[20-23]</sup>. However, the rafting process and stress distribution during compressive creep in novel  $L1_2$  hardened Co-Al-W superalloys (which exhibit a positive misfit<sup>[1,6]</sup>) has not been investigated in comparable detail. The misfit between the  $\gamma$  and  $\gamma'$  phases is defined as  $\delta = 2(a_{\gamma'} - a_{\gamma}) / (a_{\gamma'} + a_{\gamma})$ , where  $a_{\gamma'}$  is the lattice constant of the  $\gamma'$  phase and  $a_{\gamma}$  is that of the  $\gamma$  phase. During creep, the rafting process is accompanied by dislocation movement and stress relief<sup>[24]</sup>. In this study, compression creep tests were conducted on single crystal Co-9Al-9W specimens in order to investigate the evolution of the  $\gamma'$  morphology during creep. In particular, the work was directed to a detailed analysis of the dislocation and stacking fault distributions. They were investigated in detail to deduce their relation to the rafting process.

## **2. Experimental methods**

### *2.1. Material preparation*

The Co-9Al-9W alloy investigated (atomic percent composition) was initially produced from the elemental components by argon arc melting. The 70g button ingots produced were melted 5 times to achieve chemical homogeneity. A single crystal rod of Co-9Al-9W was obtained by directionally solidifying the ingots using a Bridgman-unit with a helical selector. This was done at Neue Materialien Bayreuth GmbH, Bayreuth, Germany. The crystallographic orientation of the rod and the absence of grain boundaries were confirmed by Electron Backscattered Diffraction (EBSD). It was found that the rod axis

deviated from the  $\langle 001 \rangle$  crystallographic orientation by less than  $10^\circ$  and that no grain boundaries were present. The single crystal rod was solution treated at  $1300^\circ\text{C}$  for 12 h in a vacuum furnace and cooled in the furnace to room temperature. Subsequent aging treatment was performed at  $900^\circ\text{C}$  for 200 h and finally the material was cooled in air. The heat-treatment temperatures were based on the melting points and  $\gamma'$  solvus temperatures reported in [25]. Cylindrical specimens with a diameter of 5 mm and a length of 7.5 mm for compression creep tests were produced by spark erosion and a subsequent grinding. The specimen axis and direction of externally applied stress of the creep tests was parallel to the  $[001]$  orientation.

## 2.2. Creep tests

The creep tests were carried out in a Satec Systems constant load machine with a lever arm ratio of 16:1. The tests were performed in air, at  $850^\circ\text{C}$  with a compressive stress of 460 MPa. The creep tests were stopped after different times and strains in order to investigate the microstructures in different creep stages. One creep test was stopped before the minimum strain rate was reached ( $\epsilon=0.07\%$ ), one at the minimum strain rate ( $\epsilon=0.4\%$ ), one after the minimum strain rate ( $\epsilon=1.2\%$ ) and one well into the third creep stage ( $\epsilon=3\%$ ), respectively[26]. The test specimens were cooled down under load to preserve the deformed micro- and dislocation structures. The crept specimens were investigated using EBSD to find the  $[010]$  and  $[100]$  orientations. Subsequently, the specimens were cut along the  $(001)$  crystallographic plane which is normal to the stress axis, as well as along the  $(010)$  or  $(100)$  crystallographic planes in order to image the microstructure on both transverse and longitudinal sections of the cylinders.

## 2.3. Microstructural characterization

Both the transverse and longitudinal sections of the crept specimens were ground and then electro polished using a solution of 35.8Vol.% 2-butanol and 2.6Vol.% perchloric acid in 61.6Vol.% methanol for 90 s at  $-41^\circ\text{C}$  with voltage of 25 V. Subsequently they were investigated by scanning electron microscope (SEM). Backscattered Electron (BSE) images as well as Electron Backscattered Diffraction (EBSD) maps were obtained using either a Leo Gemini 1530 SEM or the SEM mode of a Zeiss Auriga focused ion beam (FIB) both equipped with field emission electron guns. Transmission electron microscope (TEM) foils were cut, ground to a thickness of about  $60\ \mu\text{m}$  and subsequently electrolytically thinned to electron transparency using the Struers A3 electrolyte with a voltage of 20 V at  $-38^\circ\text{C}$ . They were then investigated using a Philips CM200 TEM operated with a voltage of 200 kV. The spatial dimensions of rafted  $\gamma'$  particles were measured from SEM images of longitudinal sections (the  $(010)$  or  $(100)$  crystallographic planes) parallel to the stress axis using the line segment intersection method in Photoshop. Four different areas of every specimen were investigated and at least 50 precipitates per area were measured to obtain average values and the standard deviation.

### 3. Results and discussion

The as aged single crystal Co-9Al-9W alloy exhibits a  $\gamma/\gamma'$  two-phase microstructure with coherently embedded cubic  $\gamma'$  precipitates as shown in Figure 1a. The original edge length of isotropic  $\gamma'$  particles varies from 100 to 200 nm. The volume fraction of  $\gamma'$  phase was measured to be about 60%. The mismatch between the  $\gamma$  and  $\gamma'$  phases in a Co-9Al-9W-0.1B alloy has been reported to be positive at room temperature and to remain positive up to 900 °C<sup>[6]</sup>. This suggests that the Co-9Al-9W alloy, with its very similar composition, would also exhibit a positive mismatch over this temperature range.

The compression creep tests performed on the single crystal Co-9Al-9W specimens (at 850 °C and 460 MPa stress) were interrupted after plastic strains of 0.4 and 3% were reached. The crept specimens interrupted at 0.4% strain, which represents the point when the minimum transient strain rate is reached, show no significant changes in the morphology of the  $\gamma'$  precipitates compared to un-crept material. They remain almost cubic as shown in Figure 1b. As the creep tests progressed further, the deformed specimens present a pronounced raft structure (see Figure 1c). This phenomenon is consistent with the results on nickel-base single crystal superalloys reported by Mantani et al.<sup>[27]</sup> who observed that significant rafting was associated with plastic deformation when the creep strain exceeded a certain threshold that was determined by the dislocation density. Due to the positive mismatch for Co-base alloys at 850 °C, the  $\gamma'$  precipitates raft perpendicularly to the external compressive stress axis. Nevertheless, the  $\gamma'$  precipitates show an almost cubic cross section when viewed on the (001) crystallographic plane normal to the stress axis as shown in Figure 1d. Some low contrast features can be discerned that are elongated and rotated by about 45° relative to the edges of the  $\gamma'$  precipitates. This is believed to be orientation contrast that results from lattice distortion due to dislocations. It was reported that dislocations in this material are of the  $a/2\langle 101 \rangle \{111\}$  type and operate in the horizontal matrix channels perpendicular to the stress axis<sup>[6,25]</sup>. The traces of such dislocations should appear under the angles observed in this micrograph. The degree of rafting is quantified as the horizontal length of  $\gamma'$  particles and width of horizontal  $\gamma$  matrix channels in Figure 1e. Part of the data in Figure 1e have already been reported in an earlier publication<sup>[26]</sup>. The elongation of  $\gamma'$  precipitates to a measurable degree started after the minimum strain rate was attained, while broadening of the horizontal  $\gamma$  channels took place predominantly during the primary creep stage. This is most easily explained by the fact that the degree of rafting when measured using the length of the  $\gamma'$  precipitates increased significantly and abruptly at the point when the  $\gamma'$  precipitates started to merge. However the increase in width of the horizontal  $\gamma$  matrix channels, which is a diffusion-controlled coarsening, is a continuous process that starts at the beginning of creep deformation. A similar behavior is also reported for nickel-base superalloys<sup>[18]</sup>.

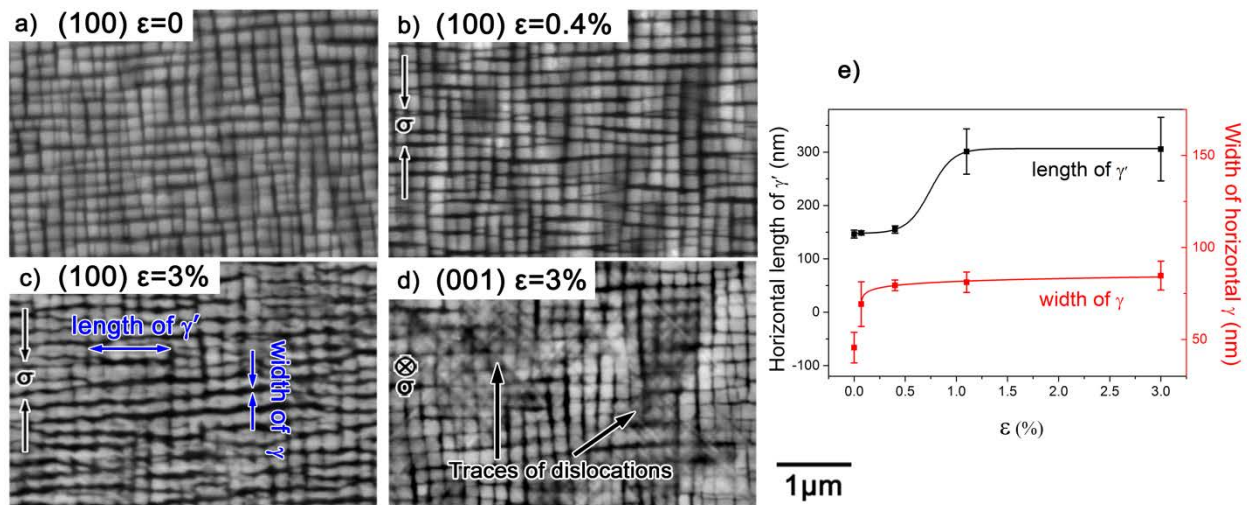


Figure 1. (a) BSE images of as aged  $\gamma/\gamma'$  two-phase microstructures; (b-c) evolution of the  $\gamma/\gamma'$  two-phase microstructure during creep, imaged in the plane parallel to the applied stress axis; (d) Traces of dislocations observed in the plane normal to the stress axis; (e) variation of the horizontal length of  $\gamma'$  precipitates and the width of the horizontal  $\gamma$  matrix channels with creep strain.

Details of the dislocation structure and the  $\gamma/\gamma'$  microstructural development, investigated by TEM, are shown in Figure 2. At a small strain (0.4%), the shape of the  $\gamma'$  precipitates remained cubic when viewed along the  $[100]$  direction, while the horizontal  $\gamma$  matrix channels perpendicular to the applied stress axis became slightly broader. Many stacking faults formed in both transverse and longitudinal sections during this primary creep stage. Several nearly straight dislocations are visible when the micrograph is taken parallel to the stress axis (see Figure 2c). At a strain of 3%, the morphology of the  $\gamma'$  precipitates had changed. The  $\gamma'$  precipitates rafted strongly along the  $[010]$  direction, which was perpendicular to the stress axis, as shown in Figure 2b, and the  $\gamma$  matrix channels perpendicular to the stress axis broadened further. Most of the  $\gamma'$  precipitates just elongated and connected with each other. Nevertheless, the positions where two former  $\gamma'$  cubes grew together are still clearly discernable being slightly thinner than the average thickness of the raft and sometimes containing small islands of matrix phase enclosed in the  $\gamma'$  raft. The  $\gamma'$  precipitates still appear in their cubic cross section when viewed along the  $[001]$  direction as shown in Figure 2d. In addition, a large number of stacking faults formed in the  $\gamma'$  precipitates. In accordance with what is reported in the literature, these were most likely formed by  $a/3\langle 112 \rangle\{111\}$  superpartial dislocations shearing the  $\gamma'$  precipitates and leaving superlattice intrinsic stacking faults (SISFs)<sup>[6]</sup>. It is notable that the stacking faults not only formed within the  $\gamma'$  precipitates but also in the  $\gamma$  matrix during the early creep stage, as marked in Figure 2a. However, as the rafting process proceeds, the number of stacking faults in the  $\gamma$  matrix channels obviously decreased (see Figure 2b). It was reported that the  $\gamma'$  precipitates are susceptible

to cutting by partial dislocations in these novel Co-base superalloys<sup>[28]</sup>. Cutting of precipitates by partial dislocations takes already place before well-developed dislocation networks and rafting are recognized in the material. The fact that stacking faults are also found throughout the  $\gamma$  matrix channels indicates that the stacking fault energies of both  $\gamma$  and  $\gamma'$  phases are low compared with nickel-base alloys. The reason why fewer stacking faults were found in the  $\gamma$  matrix after rafting took place in the later stages of creep of the Co-base alloy will be discussed in more detail later.

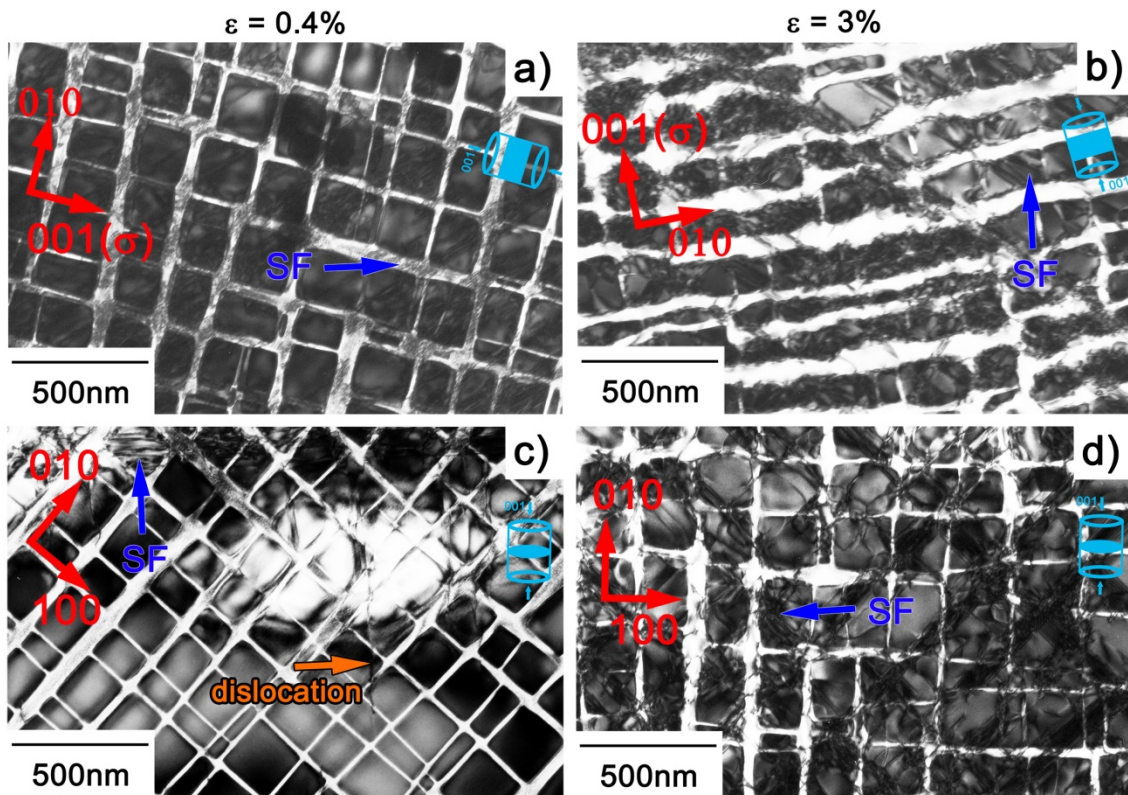


Figure 2. TEM micrographs of crept specimens, the external stress axis was along the [001] direction. (a, b) TEM foils parallel to the stress axis; (c, d) TEM foils normal to the stress axis. (a, c)  $\epsilon=0.4\%$ ; (b, d)  $\epsilon=3\%$ . SF = stacking fault.

Details of the dislocation structures and stacking faults in both the (100) and (001) crystallographic planes are shown in Figure 3. When viewed perpendicular to the stress axis, Figure 3a (i.e. nearly along [100]), the dislocations concentrate only at horizontal  $\gamma/\gamma'$  interfaces that are parallel to the rafting direction, while the vertical interfaces are nearly free of dislocations. When viewed along the stress axis, Figure 3b (i.e. along the [001] direction), the dislocation segments in some cases clearly span over a number of  $\gamma'$  particles and  $\gamma$  channels. The difference in the dislocation population of these two matrix channels

orientations is related to the different local stress states. The coherency stresses in the  $\gamma$  channels, induced by the positive misfit, are of a tensile character along the  $\gamma/\gamma'$  interfaces. Thus, the overall stress state in the horizontal channels has a compressive component perpendicular to the  $\gamma/\gamma'$  interfaces which reinforces the applied compressive stress along the [001] orientation. Therefore, the dislocations preferably move in the horizontal channels as shown in Figure 1b and Figure 3b<sup>[6,28]</sup>. As a result, the coherency stresses at horizontal  $\gamma/\gamma'$  interfaces i.e. parallel to the (001) crystallographic plane, are partially relieved by the dislocation segments<sup>[22,23,29,30]</sup>. The loss of interfacial coherency between the  $\gamma$  and  $\gamma'$  phases during creep was also observed by Coakley et al.<sup>[30,31]</sup>. The released coherency stress at horizontal  $\gamma/\gamma'$  interfaces makes it energetically beneficial that  $\gamma'$  precipitates coalesce over the less deformed vertical  $\gamma$  channels where coherency stresses are still present.

It is interesting to consider how popular alloying elements as Ta and Ti, which are added to increase the  $\gamma'$  solvus temperature and Ni, which is beneficial for  $\gamma'$  stability, affect the lattice misfit and accordingly the rafting behaviour. It was reported that the addition of both Ta and Ti could increase the positive lattice misfit between  $\gamma$  and  $\gamma'$  further. However, Ni hardly affected the misfit in Co–Al–W–Ni quaternary alloys<sup>[32]</sup>. Thus, it can be assumed that the addition of Ta and Ti promotes an earlier formation of dislocation networks and accelerates the rafting of  $\gamma'$  precipitates during creep due to an increased lattice misfit and resulting higher coherency stresses. The addition of Ni on the contrary should effect the rafting behavior much less due to Ni's weaker influence on the lattice misfit.

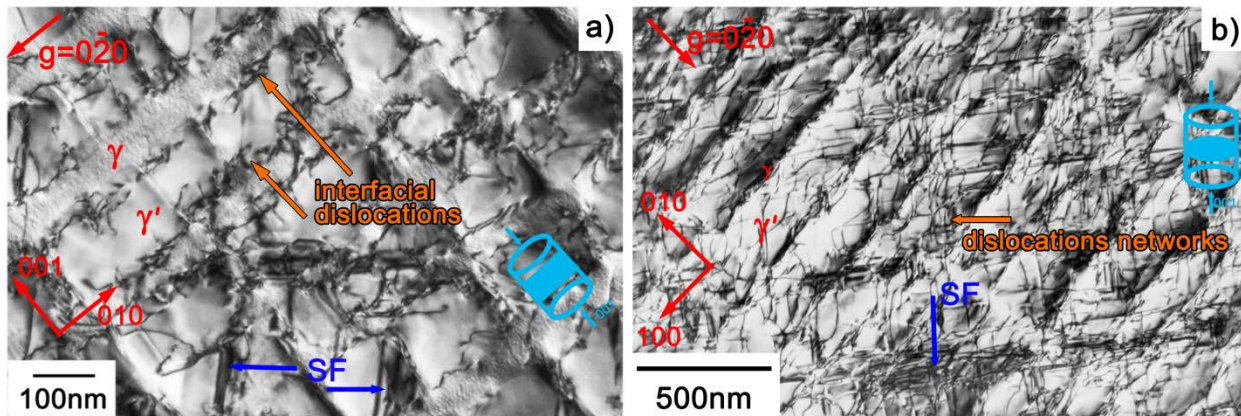


Figure 3. Two-beam dark field images of crept microstructure,  $\epsilon=3\%$ . a) Dislocation segments present at  $\gamma/\gamma'$  interfaces, beam direction near to [100] with  $g=0\bar{2}0$ ; (b) Dislocation networks in the horizontal matrix channels, beam direction near to [001] with  $g=0\bar{2}0$ .

Figure 4a is a detailed TEM image showing the merging of  $\gamma'$  precipitates on a section parallel to the external stress axis. It can be seen that adjacent  $\gamma'$  particles have started to connect together along the rafting direction. The junctions always developed first at the corners of the  $\gamma'$  precipitates at interfaces that are

parallel to the stress axis. It is striking that these corner junctions are frequently associated with stacking faults inside the  $\gamma'$  precipitates. Figure 4b shows the ribbon-like arrangement of stacking faults generated by the cutting of  $\gamma'$  precipitates and adjacent  $\gamma$  matrix channels during the early stages of creep. In the primary creep regime, the stacking faults span the  $\gamma'$  precipitates and the  $\gamma$  matrix channels, which has been shown in Figure 2a. During further creep deformation and the onset of the rafting process, the consecutive stacking faults are cut into intersecting narrow faults confined within the  $\gamma'$  precipitates as shown in Fig. 4a. It is known that the rafting process has to be accompanied by directional diffusion<sup>[18,25,33-35]</sup>. Moreover, the shearing of the  $\gamma'$  precipitates by partial dislocations, forming stacking faults, was also reported to involve local diffusion and reordering processes<sup>[36,37]</sup>. Therefore, it is reasonable to believe that the stacking faults can act as diffusion channels for the preferential merging at the corners of  $\gamma'$  particles, where the stacking faults concentrate. Viswanathan et al.<sup>[38]</sup> found that the diffusion of elements occurred along the stacking faults in nickel-base superalloys and a similar mode of stacking fault assisted diffusion can be assumed in the crystallographically similar Co-Al-W alloys.

The merging at precipitate corners during the early period of rafting creates pockets of matrix phase between the junctions, which will shrink and disappear gradually as the rafting process proceeds further. The occurrence of these pockets could influence the diffusion processes necessary for the re-distribution of alloying elements enriched in the matrix (Co) and in the  $\gamma'$  phase (Al and W) during the rafting process. All necessary diffusion processes have to take place through the ordered  $\gamma'$  phase with an L1<sub>2</sub> structure. Diffusion within such ordered crystal structures is normally slower than in unordered solid solution phases, which could decelerate the rafting process.

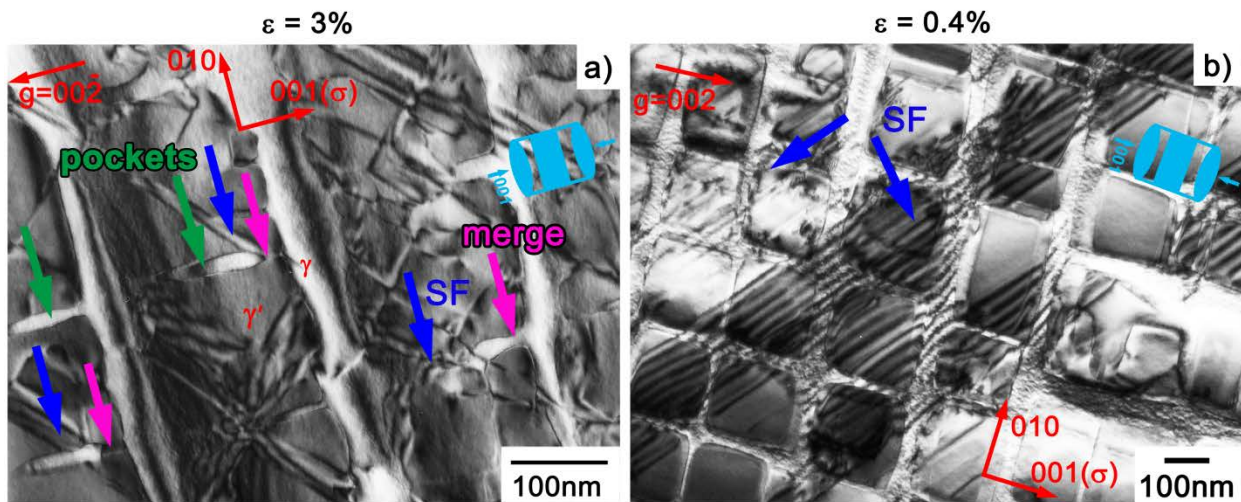


Figure 4. Two-beam dark field images of creep microstructure, beam direction near [100],  $g=00\cdot2$ . (a)  $\epsilon=3\%$ , the  $\gamma'$  precipitates merge together at the corners where stacking faults exist; (b)  $\epsilon=0.4\%$ , continuous stacking fault ribbons in the early stage of creep deformation.

It is observed that planar faults more frequently span over the  $\gamma'$  precipitates and  $\gamma$  matrix channels in the early stage of creep deformation while planar faults are more often confined within the  $\gamma'$  particles in the later stages of creep. To acquire a deeper insight into these phenomena it is instructive to consider the literature about creep deformation in polycrystalline nickel-base superalloys<sup>[36-43]</sup>. During creep, polycrystalline nickel-base superalloys exhibit stacking fault arrangements very similar to the ones found in the Co-Al-W alloy investigated in the current work. They are generated by the motion of partial and superpartial dislocations of the  $a/6\langle 112 \rangle$  and  $a/3\langle 112 \rangle$  types. The partial and superpartial dislocations are the result of dislocation decomposition processes of ordinary and superdislocations and they move through the alloy in either a correlated or uncorrelated manner. While the correlated movement results in planar faults that are confined to the  $\gamma'$  particles, the uncorrelated movement generates stacking fault ribbons spanning over both the  $\gamma'$  particles and the  $\gamma$  matrix phase in between. The different dislocation and planar fault configurations found, or under discussion, in polycrystalline nickel-base superalloys are manifold. It is beyond the scope of the present work as to whether and to which extent exactly similar configurations are present in ternary Co-Al-W alloys. Nevertheless, it is noteworthy that the transition from correlated dislocation movement to uncorrelated dislocation movement in nickel-base superalloys is connected with the microstructure, i.e. the fraction, size distribution and distance between the  $\gamma'$  particles. A low volume fraction of widely separated  $\gamma'$  particles favours correlated dislocation movement generating planar faults confined to  $\gamma'$  particles. Closely spaced  $\gamma'$  particles promoted uncorrelated movement of partial dislocations with a trailing stacking fault ribbon spanning over the matrix and  $\gamma'$  particles<sup>[43]</sup>. In Co-Al-W alloys rafting takes place during creep and results in an increasing width of horizontal  $\gamma$  channels. It is assumed that the relatively narrow matrix channels at the onset and during the initial stages of creep favour uncorrelated movement of partial dislocations while in the later stages of creep, when the  $\gamma$  matrix channels have widened, a correlated movement of dislocations in the matrix phase is favoured. Complete dislocations in the matrix phase and movement of (super)partial dislocations in the  $\gamma'$  particles which generate stacking faults is associated with the latter deformation mechanism; as also observed by Titus et al.<sup>[44]</sup>. However it has to be mentioned that these authors do not report any influence of the microstructure on the dislocation configuration, which, in the present work, is assumed to explain the transition from mostly extended stacking fault ribbons to mostly planar faults confined within the  $\gamma'$  particles. To conclude, further in depth investigations are necessary to fully reveal the modes of plastic creep deformation in these ternary Co-Al-W-alloys.

#### 4. Conclusions

- The  $\gamma'$  precipitates directionally coarsen perpendicular to the external stress axis during compressive creep. This is due to the positive misfit at the test temperature of 850 °C.
- The rafting of  $\gamma'$  precipitates started after the minimum strain rate was reached.
- Dislocations preferentially move in the horizontal matrix channels normal to the stress axis and relieve the coherency stress at  $\gamma/\gamma'$  interfaces perpendicular to the external stress axis. The combination of applied and coherency stress is the driving force for rafting.
- The merging of  $\gamma'$  precipitates during rafting starts at the particle corners where stacking faults are present, leaving pockets of matrix phase in the vertical  $\gamma$  channels between adjacent  $\gamma'$  particles. The stacking faults may act as easy diffusion paths through the ordered  $\gamma'$  phase.
- The ribbon-like stacking faults formed during the primary creep stage span over both  $\gamma$  channels and  $\gamma'$  precipitates. With ongoing rafting, planar faults are found to be confined within the  $\gamma'$  precipitates.

#### Acknowledgements

Yuzhi Li acknowledges the funding from the China Scholarship Council program (201306290056). This work was partly supported by the National Natural Science Foundation of China (No.51775440).

#### References

- [1] A. Suzuki, G.C. DeNolf, T.M. Pollock. Flow stress anomalies in  $\gamma/\gamma'$  two-phase Co–Al–W–base alloys. *Scripta Materialia*. 2007, 56(5): 385~388
- [2] C.T. Sims, N.S. Stoloff, W.C. Hagel. *superalloys II*. 1987,
- [3] Y. Li, F. Pyczak, M. Oehring, L. Wang, J. Paul, U. Lorenz, Z. Yao. Thermal stability of  $\gamma'$  phase in long-term aged Co-Al-W alloys. *Journal of Alloys and Compounds*. 2017, 729: 266~276
- [4] J. Sato. Cobalt-base high-temperature alloys. *Science*. 2006, 312(5770): 90~91
- [5] M.S. Titus, A. Suzuki, T.M. Pollock. Creep and directional coarsening in single crystals of new  $\gamma$ - $\gamma'$  cobalt-base alloys. *Scripta Materialia*. 2012, 66(8): 574~577
- [6] F. Pyczak, A. Bauer, M. Göken, S. Neumeier, U. Lorenz, M. Oehring, N. Schell, A. Schreyer, A. Stark, F. Symanzik. Plastic deformation mechanisms in a crept L1<sub>2</sub> hardened Co-base superalloy. *Materials Science and Engineering: A*. 2013, 571(12): 13~18
- [7] A. Bauer, S. Neumeier, F. Pyczak, M. Göken. Microstructure and creep strength of different

- $\gamma/\gamma'$ -strengthened Co-base superalloy variants. *Scripta Materialia*. 2010, 63(12): 1197~1200
- [8] H. Chinen, J. Sato, T. Omori, K. Oikawa, I. Ohnuma, R. Kainuma, K. Ishida. New ternary compound  $\text{Co}_3(\text{Ge}, \text{W})$  with  $L1_2$  structure. *Scripta Materialia*. 2007, 56(2): 141~143
- [9] T.M. Pollock, J. Dibbern, M. Tsunekane, J. Zhu, A. Suzuki. New Co-based  $\gamma$ - $\gamma'$  high-temperature alloys. *Jom*. 2010, 62(1): 58~63
- [10] M. Tsunekane, A. Suzuki, T.M. Pollock. Single-crystal solidification of new Co–Al–W-base alloys. *Intermetallics*. 2011, 19(5): 636~643
- [11] V. Kuzucu, M. Ceylan, H. Elik, Aksoy. Phase investigation of a cobalt base alloy containing Cr, Ni, W and C. 1998, 74(1): 137~141
- [12] D.L. Klarstrom. Wrought cobalt-base superalloys. *Journal of Materials Engineering and Performance*. 1993, 2(4): 523~530
- [13] A. Suzuki. High-temperature strength and deformation of  $\gamma/\gamma'$  two-phase Co–Al–W-base alloys. *Acta Materialia*. 2008, 56(6): 1288~1297
- [14] A.J. Huis In't Veld, G. Boom, P.M. Bronsveld, J.T.M. de Hosson. Superlattice intrinsic stacking faults in  $\gamma'$  precipitates. *Scripta metallurgica*. 1985, 19(9): 1123~1128
- [15] Y.F. Gu, C. Cui, D. Ping, H. Harada, T. Fukuda, J. Fujioka. Creep behavior of new kinds of Ni–Co-base superalloys. *Materials Science and Engineering: A*. 2009, 510: 250~255
- [16] A. Pineau. Influence of uniaxial stress on the morphology of coherent precipitates during coarsening—elastic energy considerations. *Acta metallurgica*. 1976, 24(6): 559~564
- [17] S.G. Tian, H.H. Zhou, J.H. Zhang, H.C. Yang, Y.B. Xu, Z.Q. Hu. Directional coarsening of  $\gamma'$  phase in single crystal nickel based superalloys during tensile creep. *Materials Science and Technology*. 2000, 16(4): 451~456
- [18] T.M. Pollock, A.S. Argon. Directional coarsening in nickel-base single crystals with high volume fractions of coherent precipitates. *Acta metallurgica et materialia*. 1994, 42(6): 1859~1874
- [19] F. Pyczak, A. Bauer, M. Göken, U. Lorenz, S. Neumeier, M. Oehring, J. Paul, N. Schell, A. Schreyer, A. Stark, F. Symanzik. The effect of tungsten content on the properties of  $L1_2$ -hardened Co–Al–W alloys. *Journal of Alloys and Compounds*. 2015, 632: 110~115
- [20] J.Y. Buffiere, M. Ignat. A dislocation based criterion for the raft formation in nickel-based superalloys single crystals. *Acta metallurgica et materialia*. 1995, 43(5): 1791~1797
- [21] A. Epishin, T. Link, U. Brückner, P.D. Portella. Kinetics of the topological inversion of the

- $\gamma/\gamma'$ -microstructure during creep of a nickel-based superalloy. *Acta Materialia*. 2001, 49(19): 4017~4023
- [22] T.M. Pollock, A.S. Argon. Creep resistance of CMSX-3 nickel base superalloy single crystals. *Acta Metallurgica et Materialia*. 1992, 40(1): 1~30
- [23] H. Mughrabi, U. Tetzlaff. Microstructure and high-temperature strength of monocrystalline nickel-base superalloys. *Advanced Engineering Materials*. 2000, 2(6): 319~326
- [24] R.C. Reed, D.C. Cox, C.M.F. Rae. Kinetics of rafting in a single crystal superalloy: effects of residual microsegregation. 2007, 23(8): 893~902
- [25] A. Bauer, S. Neumeier, F. Pyczak, M. Göken. Creep strength and microstructure of polycrystalline  $\gamma'$ -strengthened cobalt-base superalloys. *Superalloys 2012*. 2012: 695~703
- [26] Y. Li, F. Pyczak, J. Paul, M. Oehring, U. Lorenz, Z. Yao. Microstructure evolution in  $L_{12}$  hardened Co-base superalloys during creep. *Journal of Materials Research*. 2017, 32(24): 4522~4530
- [27] N. Matan, D.C. Cox, C. Rae, R.C. Reed. On the kinetics of rafting in CMSX-4 superalloy single crystals. *Acta Materialia*. 1999, 47(7): 2031~2045
- [28] K. Tanaka, T. Ohashi, K. Kishida, H. Inui. Single-crystal elastic constants of  $Co_3(Al,W)$  with the  $L_{12}$  structure. *Applied Physics Letters*. 2007, 91(18): 181907
- [29] S. Ma, L. Carroll, T.M. Pollock. Development of  $\gamma$  phase stacking faults during high temperature creep of Ru-containing single crystal superalloys. *Acta Materialia*. 2007, 55(17): 5802~5812
- [30] K. Tanaka, M. Ooshima, N. Tsuno, A. Sato, H. Inui. Creep deformation of single crystals of new Co-Al-W-based alloys with fcc/ $L_{12}$  two-phase microstructures. *Philosophical Magazine*. 2012, 92(32): 4011~4027
- [31] J. Coakley, E.A. Lass, D. Ma, M. Frost, H.J. Stone, D.N. Seidman, D.C. Dunand. Lattice parameter misfit evolution during creep of a cobalt-based superalloy single crystal with cuboidal and rafted gamma-prime microstructures. *Acta Materialia*. 2017, 136: 118~125
- [32] H. Yan, V.A. Vorontsov, J. Coakley, N.G. Jones, H.J. Stone, D. Dye. Quaternary alloying effects and the prospects for a new generation of Co-base superalloys. *Superalloys 2012*. 2012: 705~714
- [33] I.L. Svetlov, B.A. Golovko, A.I. Epishin, N.P. Abalakin. Diffusional mechanism of gamma-prime-phase particle coalescence in single crystals of nickel-base superalloys. *Scripta*

Metallurgica et Materialia;(United States). 1992, 26

- [34] J.Y. Buffiere, M.C. Cheynet, M. Ignat. Stem analysis of the local chemical composition in the nickel-based superalloy CMSX-2 after creep at high temperature. *Scripta Materialia*. 1996, 34(3)
- [35] M. Saito, T. Aoyama, K. Hidaka, H. Tamaki, T. Ohashi, S. Nakamura, T. Suzuki. Concentration profiles and the rafting mechanism of Ni base superalloys in the initial stage of high temperature creep tests. *Scripta Materialia*. 1996, 34(8)
- [36] L. Kovarik, R.R. Unocic, J. Li, M.J. Mills. The intermediate temperature deformation of Ni-based superalloys: Importance of reordering. *Jom*. 2009, 61(2): 42~48
- [37] V.A. Vorontsov, L. Kovarik, M.J. Mills, C. Rae. High-resolution electron microscopy of dislocation ribbons in a CMSX-4 superalloy single crystal. *Acta Materialia*. 2012, 60(12): 4866~4878
- [38] G.B. Viswanathan, R. Shi, A. Genc, V.A. Vorontsov, L. Kovarik, C.M.F. Rae, M.J. Mills. Segregation at stacking faults within the  $\gamma'$  phase of two Ni-base superalloys following intermediate temperature creep. *Scripta Materialia*. 2015, 94: 5~8
- [39] B. Decamps, S. Raujol, A. Coujou, F. Pettinari-Sturmel, N. Clement, D. Locq, P. Caron. On the shearing mechanism of  $\gamma'$  precipitates by a single  $(a/6)\langle 112 \rangle$  Shockley partial in Ni-based superalloys. *Philosophical Magazine*. 2004, 84(1): 91~107
- [40] L. Kovarik, R.R. Unocic, J. Li, P. Sarosi, C. Shen, Y. Wang, M.A.D.T. Mills, M. Benyoucef, D. Locq, P. Caron, F. Pettinari, N. Clément, A.J.P.M. Coujou. Microtwinning and other shearing mechanisms at intermediate temperatures in Ni-based superalloys. *Progress in Materials Science*. 2009, 54(6): 839~873
- [41] S. Raujol, M. Benyoucef, D. Locq, P. Caron, F. Pettinari, N. Clément, A. Coujou. Decorrelated movements of Shockley partial dislocations in the  $\gamma$ -phase channels of nickel-based superalloys at intermediate temperature. *Philosophical Magazine*. 2006, 86(9): 1189~1200
- [42] R.R. Unocic, G.B. Viswanathan, P.M. Sarosi, S. Karthikeyan, J. Li, M.J. Mills. Mechanisms of creep deformation in polycrystalline Ni-base disk superalloys. *Materials Science and Engineering: A*. 2008, 483: 25~32
- [43] G.B. Viswanathan, P.M. Sarosi, M.F. Henry, D.D. Whitis, W.W. Milligan, M.J. Mills. Investigation of creep deformation mechanisms at intermediate temperatures in René 88 DT.

Acta Materialia. 2005, 53(10): 3041~3057

[44] M.S. Titus, Y.M. Eggeler, A. Suzuki, T.M. Pollock. Creep-induced planar defects in L1<sub>2</sub>-containing Co- and CoNi-base single-crystal superalloys. Acta Materialia. 2015, 82: 530~539